# Modes and the alpha-gamma transition in rf capacitive discharges in $N_2O$ at different rf frequencies

V. Lisovskiy[a)]
*Laboratoire de Physique et Technologie des Plasmas, Ecole Polytechnique, Palaiseau 91128, France and Kharkov National University, Kharkov 61077, Ukraine*

J.-P. Booth
*Laboratoire de Physique et Technologie des Plasmas, Ecole Polytechnique, Palaiseau 91128, France*

K. Landry, D. Douai, and V. Cassagne
*Unaxis Displays Division France SAS, 5, Rue Leon Blum, Palaiseau 91120, France*

V. Yegorenkov
*Kharkov National University, Kharkov 61077, Ukraine*

(Received 7 August 2006; accepted 25 September 2006; published online 31 October 2006)

This paper reports current-voltage characteristics and pressure-voltage transition curves from the weak-current $\alpha$-mode to the strong-current $\gamma$-mode for rf capacitive discharges in $N_2O$ at frequencies of 2 MHz, 13.56 MHz, and 27.12 MHz. At 2 MHz the rf discharge is mostly resistive whereas at 13.56 MHz and 27.12 MHz it is mostly capacitive. The weak-current $\alpha$-mode was found to exist only above a certain minimum gas pressure for all frequencies studied. N. Yatsenko [Sov. Phys. Tech. Phys. **26**, 678 (1981)] previously proposed that the $\alpha-\gamma$ transition corresponds to breakdown of the sheaths. However, we show that this is the case only for sufficiently high gas pressures. At lower pressure there is a smooth transition from the weak-current $\alpha$-mode to a strong-current $\gamma$-mode, in which the sheaths produce fast electrons but the sheath has not undergone breakdown. © *2006 American Institute of Physics*. [DOI: 10.1063/1.2364135]

## I. INTRODUCTION

rf capacitive discharges in $N_2O$ are commonly used for cleaning silicon wafers, for oxidizing silicon surfaces,[1] as well as for producing oxynitride films on silicon.[2] Oxynitrides have good electrical properties (high breakdown voltage, reliability, improved current-voltage, and optical characteristics),[2] permitting them to be used as active layers in semiconductors, memory devices, and chemical sensors.[3] These amorphous films ($a$-$SiN_xO_y$ and $a$-$SiN_xO_y$:H) are produced in rf discharges in a $N_2O/SiH_4$ (silane) mixture,[3–7] the oxynitride film being deposited on the substrate surface rather than formed by oxidation and nitridation of the material. rf discharges in $N_2O/SiH_4$ mixtures are also used for depositing $SiO_2$ films.[8–12] Typically the $N_2O$ concentration is 2–40 times higher than that of silane. Consequently, it is of considerable interest to study the properties of rf capacitive discharges in pure $N_2O$. However, published results are scarce,[13,14] and present only 3 V W characteristics together with discussions of the molecular dissociation. The process of $N_2O$ dissociation was also studied experimentally and theoretically.[15]

This paper considers the current-voltage characteristics (Ohmic current) and delivered power in a rf capacitive discharge in $N_2O$ at rf frequencies of 2 MHz, 13.56 MHz, and 27.12 MHz over a broad range of rf voltage and gas pressure. At 2 MHz and low gas pressure ($<0.2$ Torr) the discharge was found to exist only in the strong-current $\gamma$-mode, whereas the weak-current $\alpha$-mode can exist at higher $N_2O$ pressure. Furthermore, the discharge was relatively resistive, whereas at 13.56 MHz and 27.12 MHz the discharge is more capacitive. In the weak-current mode the dependence of the Ohmic current on frequency $f$ at fixed voltage can be approximated as $f^{5/3}$. The pressure-voltage curves of the $\alpha-\gamma$ transition were measured at each rf frequency. The weak-current $\alpha$-mode was found not to exist at the low-pressures side of the point where the $\alpha-\gamma$ transition curve crosses the extinction curve for all three frequencies. We investigated the $\alpha-\gamma$ transition and show that at high gas pressure the $\alpha-\gamma$ transition is accompanied by breakdown of the near-electrode sheath whereas at low gas pressure the breakdown criterion for the sheath below the $\alpha-\gamma$ transition is not met. However, in this mode the near-electrode sheaths are a source of fast electrons.

## II. EXPERIMENTAL SETUP

rf discharges were ignited in $N_2O$ over the pressure range $p \approx 0.004-5.2$ Torr with rf field frequencies $f=2$ MHz, $f=13.56$ MHz, and $f=27.12$ MHz. The distance between the flat circular aluminum electrodes (143 mm in diameter) was equal to $L=20.4$ mm. The rf voltage (amplitude $U_{rf}<1500$ V) was fed to one of the electrodes, while the other was grounded. The electrodes were located inside a fused silica tube with an inner diameter of 145 mm (see Fig. 1). The gas was supplied through small orifices in the powered electrode and then pumped out via the gap between the second electrode and the wall of the fused silica tube.

The gas pressure was monitored with 10 and 1000 Torr capacitive manometers (MKS Instruments). The gas flow

a)Electronic mail: lisovskiy@yahoo.com

 

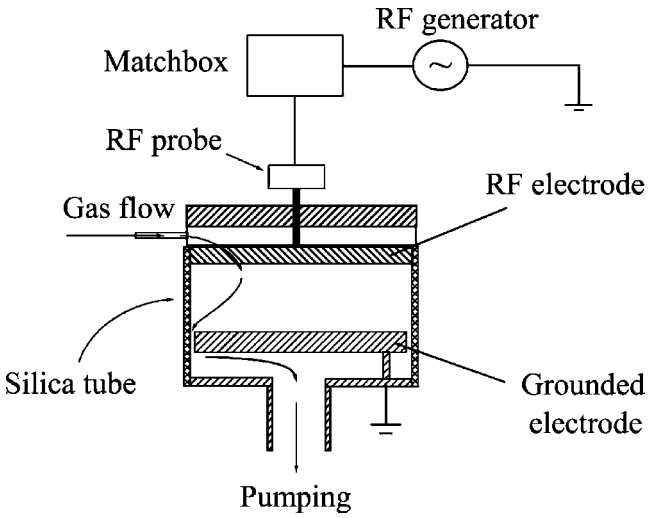


FIG. 1. Schematic of the symmetric rf discharge.

was fixed with a mass flow controller to 5 sccm, and the pressure regulated by throttling the outlet to the pump. A pressure controller (adaptive pressure controller) maintained constant gas pressure.

The rf voltage was measured with a rf current-voltage probe (Advanced Energy Z'SCAN). This rf probe was located at the minimum possible distance from the rf electrode. This probe gave measurements of the rf voltage, rf current, phase shift angle $\varphi$ between current and voltage and delivered power. The rf voltage was delivered by a 500 W rf generator rf5S (rf Power Products Inc.) via a matching box PFM (Huttinger Elektronik GmbH) of the L-type.

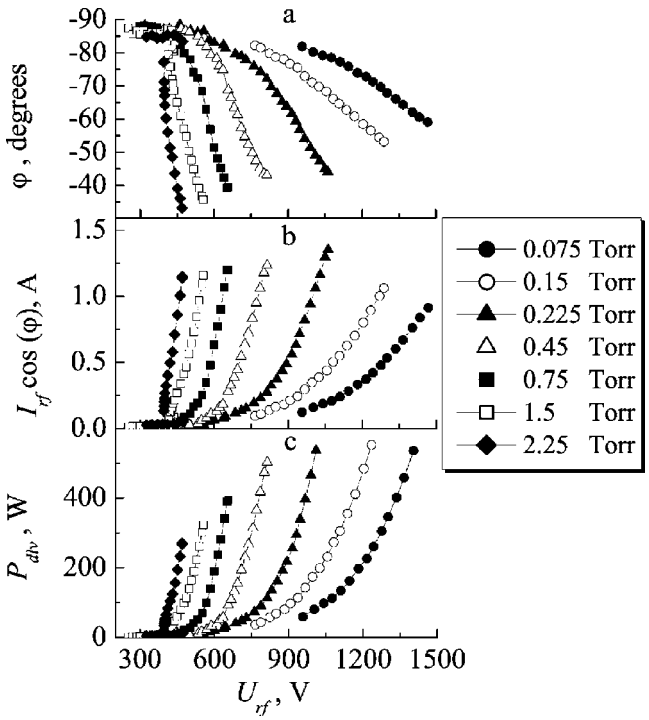


FIG. 2. The phase shift angle $\varphi$ between the rf current and voltage (a), the Ohmic rf current $I_{\mathrm{rf}}\cos\varphi$ (b) and delivered power $P_{\mathrm{dlv}}$ (c) against the rf voltage applied $U_{\mathrm{rf}}$ for the frequency value of $f=2$ MHz.

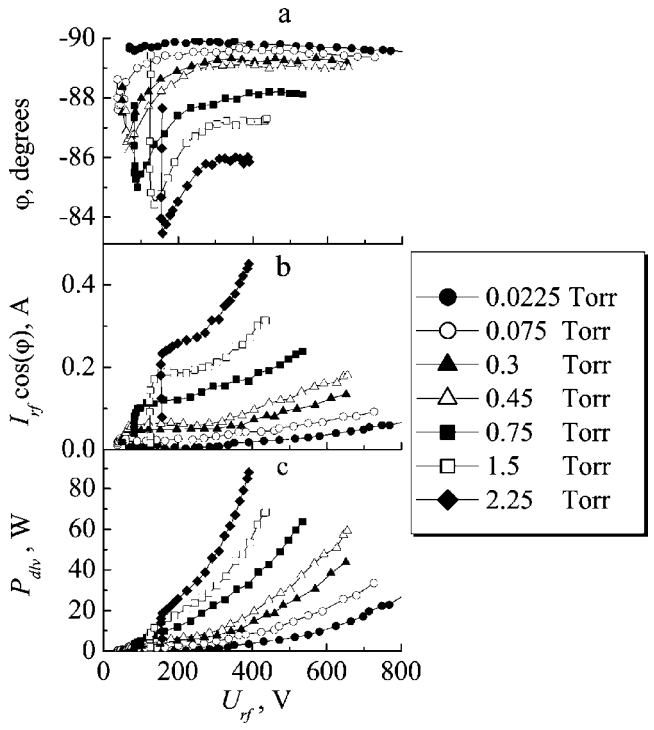


FIG. 3. The phase shift angle $\varphi$ between the rf current and voltage (a), the Ohmic rf current $I_{\mathrm{rf}}\cos\varphi$ (b) and delivered power $P_{\mathrm{dlv}}$ (c) against the rf voltage applied $U_{\mathrm{rf}}$ for the frequency value of $f=13.56$ MHz.

## III. EXPERIMENTAL RESULTS

First consider the current-voltage characteristics (CVC) and the delivered rf power at different frequencies. Figure 2 shows the phase angle, $\varphi$, between the rf current and voltage, the Ohmic rf current, $I_{\mathrm{rf}}\cos\varphi$, and the delivered power, $P_{\mathrm{dlv}}$, as a function of the applied rf voltage, $U_{\mathrm{rf}}$, at $f=2$ MHz. At this frequency, at low voltages (close to discharge extinction) the phase angle was $\varphi\approx-85°$ to $-90°$, but for higher rf voltages the absolute value of $\varphi$ decreases quickly, and the discharge becomes more resistive. We also observe a fast growth of the Ohmic rf current and the delivered power, indicating that at low gas pressure ($p<0.2$ Torr) the discharge is always in the strong-current $\gamma$-mode. At pressures above 0.22 Torr the CVC, on a logarithmic scale, shows a characteristic dogleg feature, indicating the existence of the weak-current $\alpha$-mode at low voltage. Over the entire range of gas pressure studied the discharge was in the abnormal glow regime, with the discharge luminosity completely covering the surface of the electrodes. Perhaps the normal regime would appear at higher gas pressure.

Figure 3 shows the phase angle, the Ohmic current, and the delivered power as a function of applied rf voltage at $f=13.56$ MHz. As the rf voltage is increased the absolute value of $\varphi$ first decreases, passes a minimum, then increases. After the transition from $\alpha$- to $\gamma$-mode the absolute value of $\varphi$ decreases again. In contrast to the case of $f=2$ MHz (Fig. 2), at $f=13.56$ MHz the phase angle only varies over a narrow range $\varphi\approx-83°$ to $-90°$, indicating the capacitive nature of the discharge. At pressures below 0.6 Torr the discharge was always in the abnormal regime. However, at higher gas pressure the electrode area occupied by the dis-

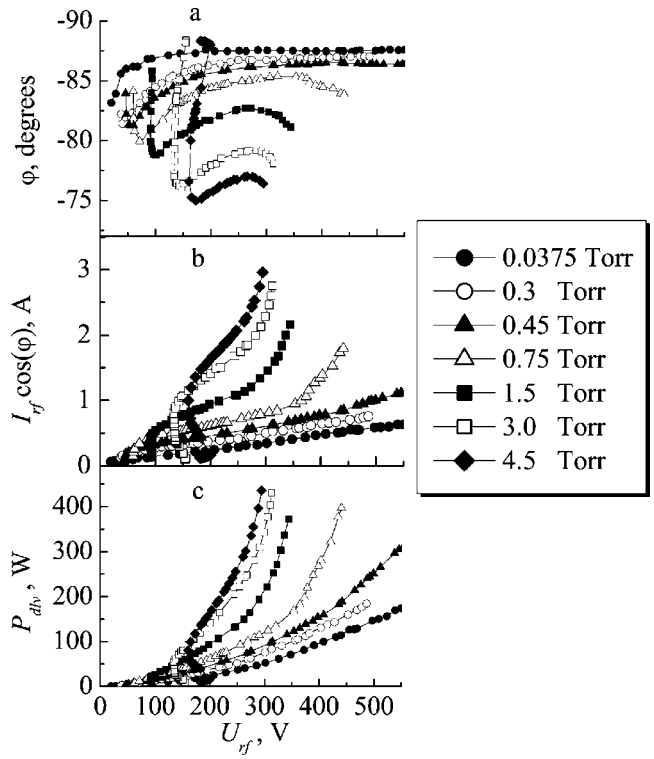


FIG. 4. The phase shift angle $\varphi$ between the rf current and voltage (a), the Ohmic rf current $I_{\mathrm{rf}}\cos\varphi$ (b) and delivered power $P_{\mathrm{dlv}}$ (c) against the rf voltage applied $U_{\mathrm{rf}}$ for the frequency value of $f=27.12$ MHz.

charge decreased as the current was decreased towards extinction, i.e., the normal regime was observed. This decrease in the discharge current and delivered power occurs at approximately constant rf voltage.

The behavior of the phase angle can be explained as follows. In the absence of a discharge the rf current is limited by the capacitive reactance of the gap between the parallel-plate electrodes, giving a phase angle $\varphi=-\pi/2$. When the discharge is present and the plasma density (consequently, the conductivity) is high, the rf current is limited by the capacitive reactance of near-electrode sheaths, depending on their thickness $d_{\mathrm{sh}}$. At low plasma density the resistance of the plasma is significant, but as the plasma density increases, the sheath thickness $d_{\mathrm{sh}}$ and its capacitive reactance change only a small amount, whereas the Ohmic resistance of the quasineutral plasma decreases considerably. Therefore, on increasing the rf voltage the phase angle again approaches a value $-\pi/2$. At moderate values of the rf voltage, when the plasma density and conductivity are small, its resistance is comparable to the capacitive impedance of the sheaths. Furthermore, the contribution of the Ohmic current to the total discharge current is at maximum, and the absolute value of the phase angle approaches a minimum value.

Figure 4 shows the phase angle, the Ohmic rf current and the delivered power as a function of the applied rf voltage at $f=27.12$ MHz. Even though the frequency has doubled, the discharge is more resistive than at 13.56 MHz. As a rule, the absolute value of the phase angle was several degrees smaller than at $f=13.56$ MHz for a comparable voltage. At low pressure ($p<0.5$ Torr) the discharge was always

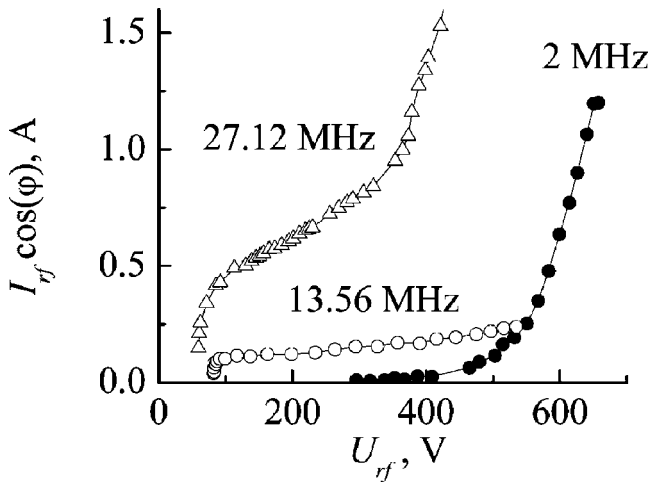


FIG. 5. The Ohmic rf current $I_{\mathrm{rf}}\cos\varphi$ against the rf voltage applied $U_{\mathrm{rf}}$ for the frequency values of 2 MHz, 13.56 MHz, and 27.12 MHz, $p=0.75$ Torr.

in the abnormal regime, whereas at higher pressure the normal regime was also observed.

At pressures above 1.5 Torr, as the current is decreased the discharge area decreases, but the voltage *increases*. Such negative differential resistance is characteristic of the subnormal regime of a dc discharge,[16] but in this case the discharge area *increases* as current is decreased.[17] Probably, at high frequency and pressures above 1.5 Torr the normal glow exists only within a narrow range of discharge current. On further decreasing the current, the decrease of the discharge area is accompanied by a reduction of the discharge current density, i.e., the plasma density. At the same time the intensity of the discharge glow was reduced a little. It would be of interest to perform detailed probe and optical studies of the normal regime close to rf discharge extinction.

Figure 5 shows the Ohmic current for a gas pressure of 0.75 Torr and frequencies of 2 MHz, 13.56 MHz, and 27.12 MHz. At this pressure the $\alpha-\gamma$ transition occurs smoothly for all three frequency values, without jumps. This transition is manifested by a dogleg feature in the CVC (logarithmic scale); the discharge glow near the sheath boundaries acquires a violet tint in the $\gamma$-mode (indicating the appearance of high energy electrons accelerated through a high voltage drop across the sheath). Furthermore, the almost uniform glow of the quasineutral plasma in the $\alpha$-mode becomes stratified after the transition to the $\gamma$-mode: an analog of a negative glow appears near the boundaries of near-electrode sheaths and a darker region appears in the center, similar to two Faraday dark spaces overlapping at the center of the discharge gap. Such a simultaneous variation of the discharge structure and the glow near the sheath boundaries, together with the dogleg feature in the CVC, were a reliable indication of the $\alpha-\gamma$ mode transition.

Figure 5 also shows that the discharge current in the weak-current mode increases with the frequency. Figure 6 presents the Ohmic rf current against the frequency for $p=0.75$ Torr and $U_{\mathrm{rf}}=300$ V. These results are satisfactorily described by the function $f^{5/3}$, predicted by Raizer *et al.*[18]

Figure 7 shows the discharge CVCs at $p=1.5$ Torr. The $\alpha-\gamma$ transition at $f=2$ MHz occurs discontinuously, with

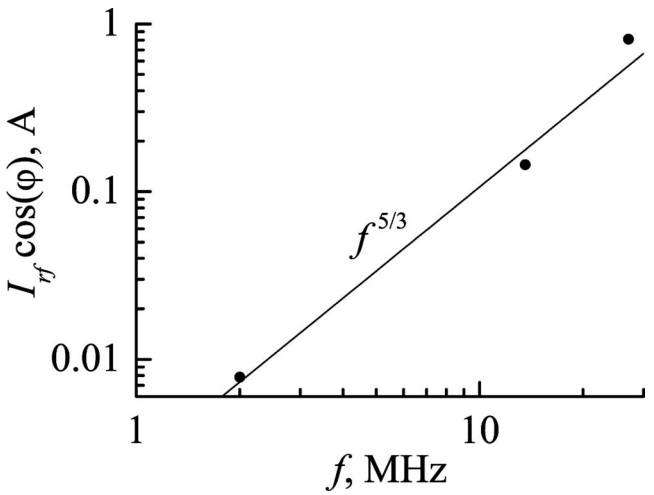


FIG. 6. The Ohmic rf current $I_{\mathrm{rf}}\cos\varphi$ against the frequency for the rf voltage applied $U_{\mathrm{rf}}=300$ V, $p=0.75$ Torr.

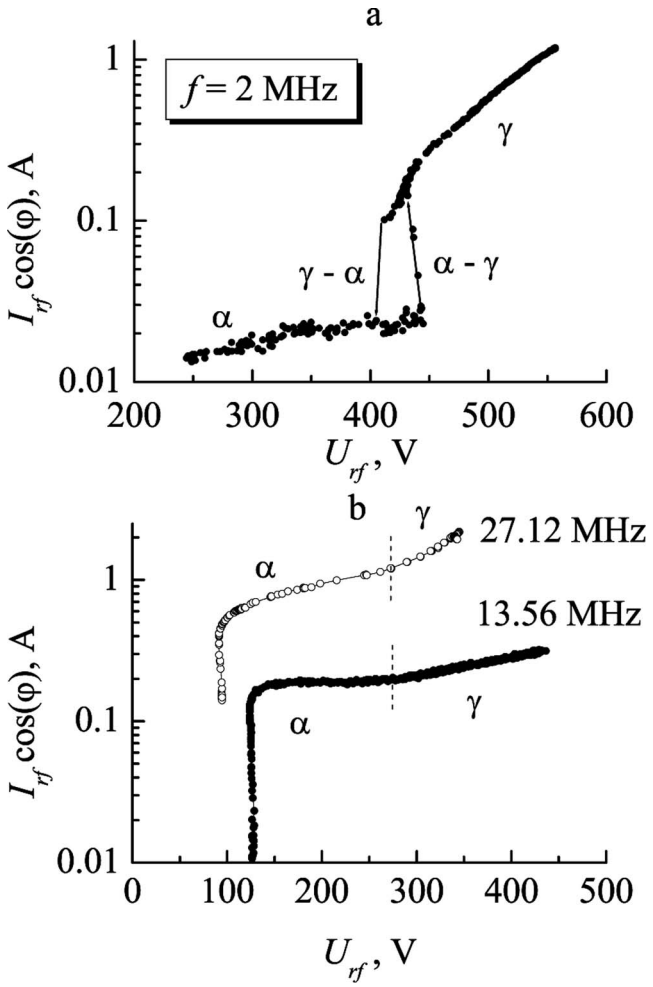


FIG. 7. The Ohmic rf current $I_{\mathrm{rf}}\cos\varphi$ against the rf voltage applied $U_{\mathrm{rf}}$ for the frequency values of 2 MHz (a), 13.56 MHz and 27.12 MHz (b), $p=1.5$ Torr.

hysteresis (the reverse $\gamma-\alpha$ transition occurs at lower rf voltage than the $\alpha-\gamma$ transition). The near-electrode sheath is thinner in the $\gamma$-mode (in the $\alpha$-mode $d_{\mathrm{sh}}\approx 7.5$ mm, whereas in the $\gamma$-mode $d_{\mathrm{sh}}\approx 6.5$ mm). At the frequencies of $f=13.56$ MHz and $f=27.12$ MHz the $\alpha-\gamma$ transition is continuous, without jumps in the discharge parameters. It also follows from Fig. 7 that, on decreasing the rf voltage towards extinction (at the smallest rf voltage values of discharge sustainment) the discharge at $f=13.56$ MHz and $f=27.12$ MHz was in the normal regime (the discharge current decreases at constant rf voltage, with a simultaneous decrease in the discharge area on the electrode). In contrast the discharge at $f=2$ MHz was in the abnormal regime, and occupied the total area of the electrodes.

Figure 8 shows the pressure-voltage extinction curves for a rf discharge in $N_2O$ at $f=2$ MHz, $f=13.56$ MHz, and $f=27.12$ MHz. As is known,[19] rf breakdown curves can possess diffusion-drift, Paschen, and multipactor branches. In a recent paper[20] it was shown that rf discharge extinction curves have shapes that are similar to those of the breakdown curves. Each branch of the breakdown curve has its analog in the extinction curve. At a fixed rf frequency and for narrow gaps ($<10$ mm) the diffusion-drift branch is weakly expressed or not observed (for pressures below 10 Torr), and the Paschen and multipactor branches dominate.[21] Correspondingly, the extinction curve under these conditions also possesses analogs of the Paschen and multipactor branches and the branch corresponding to the diffusion-drift branch of the breakdown curve may be absent. We observe this behavior in Fig. 8 at the frequency 2 MHz, where the extinction curve shows only the analog of the Paschen branch and, for the pressures below 0.15 Torr, a transition to the multipactor branch; the equivalent of the diffusion-drift branch was not observed. Increasing the frequency changes the shape of the extinction curves (and of the breakdown curves) in a similar way to increasing the interelectrode distance. In the extinction curves at $f=13.56$ MHz and $f=27.12$ MHz we observe only the equivalent of the diffusion-drift branches of the breakdown curves; the equivalents of the Paschen and multipactor branches occur for much higher rf voltages, and are not observed in Fig. 8. The left-hand branches of the extinction curves (at low gas pressure) show regions of multivalued dependence of the discharge extinction voltage on gas pressure similar to the breakdown curves.[21] Reference 20 describes why such regions appear. At higher rf frequency the multivalued region of the extinction curves becomes more clearly expressed.

Figure 8 also shows the measured $\alpha-\gamma$ transition curves $U_{\alpha\gamma.\mathrm{exp}}$, for all three frequencies. For $f=2$ MHz the $\alpha-\gamma$ transition curve exhibits a well-expressed minimum at $p\approx 1$ Torr. For pressures below 0.2 Torr the rf discharge can exist only in the strong-current $\gamma$-mode; the weak-current mode cannot exist below this gas pressure, in agreement with previous work.[24,25]

The region over which the $\alpha$-mode can exist is also bounded at the high-pressure side ($p\sim 10$ Torr: for a fixed distance between the electrodes $L$ there is a pressure $p_{\mathrm{cr}}$, which is such that at $p>p_{\mathrm{cr}}$ the rf discharge can burn only in the strong-current $\gamma$-mode).[18,22,23] At higher frequency ($f=13.56$ MHz and $f=27.12$ MHz) the $\alpha-\gamma$ transition curves are seen to approach the extinction curves at high pressures. That is, at $p\sim 10$ Torr (we did not establish the

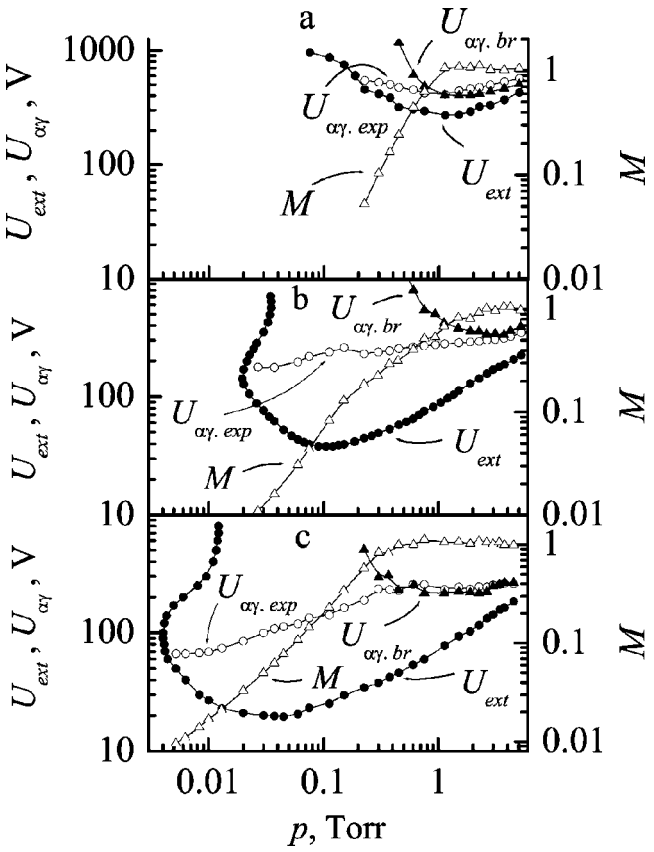


FIG. 8. The extinction curve $U_{ext}$, the $\alpha-\gamma$ transition $U_{\alpha\gamma.exp}$ experimental curve, the rf voltage of the $\alpha-\gamma$ transition $U_{\alpha\gamma.br}$, determined from criterion (7), and the quantity $M$ (4) at $f=2$ MHz (a), $f=13.56$ MHz (b) and $f=27.12$ MHz (c).

exact $p$ value as it was located outside the pressure range studied) the $\alpha-\gamma$ transition curve coincides with the extinction curve. Above this pressure the rf discharge again only exists in the strong-current $\gamma$-mode, because the rf voltage is sufficiently high to break down the narrow near-electrode sheaths.

On lowering the gas pressure the $\alpha-\gamma$ transition voltage, $U_{\alpha\gamma.exp}$, first decreases slowly then (at $p\approx0.15$ Torr for $f=13.56$ MHz and $p\approx0.3$ Torr for $f=27.12$ MHz) decreases more quickly, ultimately reaching the extinction curve. This point defines the lower pressure limit of the weak-current $\alpha$-mode (in agreement with Refs. 24 and 25).

Figure 8 also shows that increasing the frequency causes a decrease in the $\alpha-\gamma$ transition voltage. For example, at $p=3$ Torr for $f=2$ MHz we have $U_{\alpha\gamma.exp}\approx507$ V, for $f=13.56$ MHz and we obtain $U_{\alpha\gamma.exp}\approx305$ V, and for $f=27.12$ MHz the result is $U_{\alpha\gamma.exp}\approx254$ V. This result is in agreement with previous experimental[26,27] and theoretical[18,28,29] work.

## IV. MECHANISMS OF THE $\alpha-\gamma$ TRANSITION

Levitskii[30] was the first to observe that rf capacitive discharges at intermediate pressures can occur in two distinct stable regimes which he named the $\alpha$- and $\gamma$-modes after Townsend's ionization coefficients. Godyak and Khanneh[26] proposed that the $\alpha-\gamma$ transition occurs when fast electrons, produced in the sheath and penetrating into the plasma zone, generate a critical concentration of additional charge. Yatsenko[22,23] proposed that the $\alpha-\gamma$ transition corresponds to breakdown of the $\alpha$-mode sheath, determined by the same criteria which determine dc discharge breakdown (except that in his calculation $d_{sh}$, the $\alpha$-mode sheath thickness is substituted for $L$, the interelectrode separation). Here we will examine the validity of this hypothesis over a wide pressure-voltage range.

Let us first consider the motion of secondary electrons inside the near-electrode sheath. Raizer *et al.*[18] claim that in the weak-current $\alpha$-mode the time of flight of secondary electrons (ejected from the electrode surface via ion bombardment, photoemission, as well as by deactivation of metastable atoms) through the sheath is not small compared to the rf period. Following this they derived a complicated expression [see Eq. (2.20), Ref. 18, p. 75] for the parameters of the $\alpha-\gamma$ transition, describing the magnitude of the rf voltage $U_{\alpha\gamma}$ with the inclusion of the nonlinear distribution of the electric field in the sheath, oscillatory motion of the sheath boundary as well as the time of flight of a secondary electron through the sheath. As Raizer *et al.* admit, this equation contains cumbersome functions, and it is difficult to determine the condition for the $\alpha-\gamma$ transition. Let us check the validity of this claim. Consider the motion of electrons with mass $m_0$ and charge $e_0$, leaving the electrode surface and moving with a velocity $V(x)$ in the electric field $E(x)$ through a sheath of thickness $d_{sh}$

$$m_0\dot{V}=-e_0E(x)-m_0\nu_{en}V, \tag{1}$$

where $\nu_{en}$ is the rate of collisions between electrons and gas molecules. This rate can be estimated from the electron drift velocity data:[21] over the broad range $E/p=10-1000$ V/(cm Torr) one can assume $\nu_{en}/p=1.17\cdot10^{10}$ s$^{-1}$ Torr$^{-1}$. We will assume that the rf electric field $E$ decreases linearly from the electrode surface to the sheath boundary:

$$E(x)=\frac{2U_{sh}}{d_{sh}}\left(1-\frac{x}{d_{sh}}\right), \tag{2}$$

where $U_{sh}$ is the rf voltage drop across the near-electrode sheath. Then Eq. (1) can be written in the form

$$\ddot{x}=-\frac{e_0}{m_0}\frac{2U_{sh}}{d_{sh}}\left(1-\frac{x}{d_{sh}}\right)-\nu_{en}\dot{x}, \tag{3}$$

where $\ddot{x}=d^2x/dt^2$, $\dot{x}=dx/dt$, $x$ is the electron coordinate on its way through the sheath. We place the origin of the coordinate $x=0$ on the electrode surface, and assume the initial velocity of a secondary electron to be equal to zero. We can also neglect the rf voltage drop across the quasineutral plasma and regard the total voltage drop to be located within the near-electrode sheaths. This is valid, e.g., for a sufficiently dense plasma in the volume (e.g., before the $\alpha-\gamma$ transition), as well as for small interelectrode gaps and low gas pressure when the total thickness of two near-electrode sheaths is close to the interelectrode distance. Consider the cathode phase of the sheath when the thickness of one of the near-electrode sheaths is maximum (then the second sheath

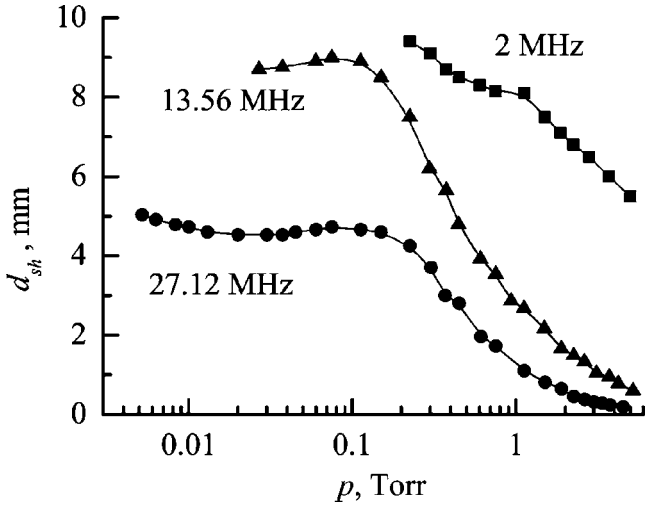


FIG. 9. The thickness of the near-electrode sheath against the gas pressure at $U_{rf}=U_{\alpha\gamma.exp}$.

is filled with electrons and it is in the anode phase), and the total rf voltage applied across the electrodes is actually located in this sheath, i.e., $U_{sh}\approx U_{rf}$.

Let us solve Eq. (3) for $f=13.56$ MHz, $p=0.027$ Torr, and $U_{rf}=177$ V, i.e., for the $\alpha-\gamma$ transition at the lowest gas pressure. The near-electrode sheath thickness was $d_{sh}\approx 8.7\pm 0.2$ mm (see Fig. 9). The time of flight of an electron through the sheath is therefore $t=1.5\cdot 10^{-9}$ s, i.e., $t/T\approx 0.02$ ($T$ is the period of the rf electric field). The relation $t\ll T$ was also found to be valid over the whole range of gas pressure, rf frequency and voltages for the $\alpha-\gamma$ transition. Probably, breakdown of the near-electrode sheath under the $\alpha-\gamma$ transition occurs at the maximum rf voltage drop across one sheath, corresponding to the maximum sheath thickness. As electron transit time in the sheath is small compared to the period $T$, we can describe the breakdown of the sheath with the DC electric field breakdown criterion [but with a nonuniform electric field distribution, $E(x)$]:

$$\gamma\left[\exp\left(\int_0^{d_{sh}}\alpha dx\right)-1\right]\equiv M=1, \tag{4}$$

$$\int_0^{d_{sh}}\alpha(x)dx=\ln\left(1+\frac{1}{\gamma}\right), \tag{5}$$

where $\gamma$ is the coefficient of ion-electron emission from the electrode surface. Let us write the first Townsend coefficient $\alpha$ in the form

$$\frac{\alpha}{p}=A\cdot\exp\left(-\frac{Bp}{E(x)}\right)=A\cdot\exp\left(-\frac{Bpd_{sh}}{2U_{rf}(1-x/d_{sh})}\right), \tag{6}$$

where $A$ and $B$ are constants. Then criterion (5) assumes the form

$$\int_0^{d_{sh}}A\cdot p\cdot\exp\left(-\frac{Bpd_{sh}}{2U_{rf}(1-x/d_{sh})}\right)dx=\ln\left(1+\frac{1}{\gamma}\right). \tag{7}$$

This expression can be written as follows:

$$\frac{AB(pd_{sh})^2}{2U_{rf}}\cdot S\left(\frac{2U_{rf}}{Bpd_{sh}}\right)=\ln\left(1+\frac{1}{\gamma}\right), \tag{8}$$

$$S(y)=\int_0^y\exp\left(-\frac{1}{t}\right)dt=\frac{y}{\exp(1/y)}-Ei\left(\frac{1}{y}\right), \tag{9}$$

where $y=2U_{rf}/(Bpd_{sh})$, $Ei$ is the integral exponent function. From (8) and (9) we obtain

$$A\cdot p\cdot d_{sh}\left[\frac{1}{\exp(Bpd_{sh}/2U_{rf})}-\frac{Bpd_{sh}}{2U_{rf}}\cdot Ei\left(\frac{Bpd_{sh}}{2U_{rf}}\right)\right]=\ln\left(1+\frac{1}{\gamma}\right). \tag{10}$$

This equation describes the rf voltage at which the breakdown of the near-electrode sheath occurs. Let us differentiate this equation with respect to $(pd_{sh})$. We find that the minimum of the $\alpha-\gamma$ transition curve $[dU_{rf}/d(pd_{sh})=0]$ is located at the rf voltage value

$$U_{rf.min}=\frac{B}{2}\frac{(pd_{sh})_{min}}{\ln(A(pd_{sh})_{min}/2\Gamma)}, \tag{11}$$

where $\Gamma=\ln[(1+\gamma)/\gamma]$. On substituting (11) in (10), we find the equation for $(pd_{sh})_{min}$

$$2\cdot\frac{A(pd_{sh})_{min}}{2\Gamma}\cdot\ln\left[\frac{A(pd_{sh})_{min}}{2\Gamma}\right]\cdot Ei\left\{\ln\left[\frac{A(pd_{sh})_{min}}{2\Gamma}\right]\right\}=1. \tag{12}$$

This equation has a solution at $A(pd_{sh})_{min}/2\Gamma=1.8454$, then

$$(pd_{sh})_{min}=\frac{2\Gamma}{A}\cdot 1.8454=3.01\cdot\frac{\Gamma}{A}=1.358\cdot e\cdot\frac{\Gamma}{A}, \tag{13}$$

where $e$ is the base of natural logarithms. Inserting (13) into (11) furnishes

$$U_{rf.min}=3.69\cdot B\cdot\frac{\Gamma}{A}=1.11\cdot e\cdot B\cdot\frac{\Gamma}{A}. \tag{14}$$

It also follows from relations (13) and (14) that

$$U_{rf.min}=0.818\cdot B\cdot(pd_{sh})_{min}. \tag{15}$$

For comparison let us write the expressions for the minimum of the dc breakdown curve:

$$(pd)_{min}=e\cdot\frac{\Gamma}{A}, \tag{16}$$

$$U_{dc.min}=e\cdot B\cdot\frac{\Gamma}{A}, \tag{17}$$

$$U_{dc.min}=B\cdot(pd)_{min}, \tag{18}$$

where $d$ is the interelectrode gap. It is clear from expressions (13)–(18) that the rf voltage at the minimum of the $\alpha-\gamma$ transition curve is 1.11 times higher than the minimum dc breakdown voltage. Correspondingly, the $(pd_{sh})_{min}$ value at the minimum of the $\alpha-\gamma$ transition curve is 1.358 times higher than the $pd$ value at the dc breakdown curve minimum. This difference is due to the nonuniformity of the elec-

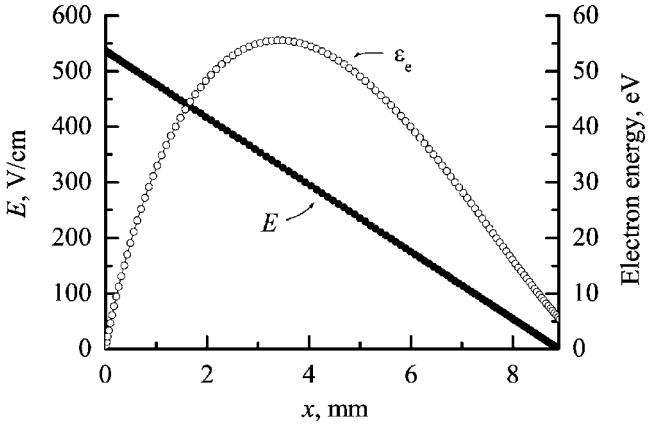


FIG. 10. The distribution of the electric field and the electron energy over the near-electrode sheath thickness, $p=0.11$ Torr, $U_{rf}=239$ V.

tric field within the rf sheath, which is maximal near the electrode and small near the sheath boundary; for dc breakdown the electric field is uniform across the entire interelectrode gap.

It follows from Figs. 8 and 9 that at $f=2$ MHz the minimum of the $\alpha-\gamma$ transition curve is located at $p=1.2$ Torr and $U_{rf}=412$ V, and the sheath thickness before the $\alpha-\gamma$ transition was $d_{sh}=8.1\pm0.2$ mm, i.e., $(pd_{sh})_{min}=0.972$ Torr·cm. To determine the values of the constants $A$ and $B$, we used the results of calculating the first Townsend coefficient $\alpha$ for $N_2O$ (Ref. 21) and got $A=21$ Torr$^{-1}$ cm$^{-1}$ and $B=450$ V/(cm Torr). Then we have from formulas (13) and (14) $(pd_{sh})_{min}=1.093$ Torr cm and $U_{rf}=401$ V. Consequently, formulas (13) and (14) furnish a satisfactory description of experimental data.

Figure 8 also shows the rf voltage of the $\alpha-\gamma$ transition $U_{\alpha\gamma.br}$, determined from criterion (7), as well as the quantity $M$ (4), calculated from the measured thickness of the sheath (see Fig. 9). The quantity $U_{\alpha\gamma.br}$ describes the rf voltage at which breakdown of the sheath occurs. It is clear from the figure that the $\alpha-\gamma$ transition only corresponds to sheath breakdown at sufficiently high gas pressure, and the $\alpha-\gamma$ transition curve $U_{\alpha\gamma.br}$ has a U-shape. In order to determine the quantity $M$ we used the measured values of the rf voltage $U_{\alpha\gamma.exp}$, at which the $\alpha-\gamma$ transition occurs. It follows from Fig. 8 that at high gas pressure (e.g., at $p>1$ Torr for the frequency $f=2$ MHz) the $U_{\alpha\gamma.exp}$ and $U_{\alpha\gamma.br}$ curves are close to each other, and just in this range the quantity $M\approx1$, i.e., the breakdown criterion holds. At lower gas pressure we have $M<1$, and the curves $U_{\alpha\gamma.exp}$ and $U_{\alpha\gamma.br}$ diverge, therefore under these conditions the $\alpha-\gamma$ transition is not accompanied by the breakdown of the near-electrode sheath.

Let us again take Eq. (3) and solve it for the $\alpha-\gamma$ transition with $f=13.56$ MHz, $p=0.11$ Torr, $U_{rf}=239$ V, and $d_{sh}\approx8.9$ mm. Figure 10 depicts the distribution of the electron energy over the near-electrode sheath thickness, which we derived from the electron velocity found from (3). At the sheath boundary the electron energy is about 6 eV, but within the sheath itself electrons have energies up to 55 eV. A portion of fast electrons having acquired high energy on passing through the sheath may approach the sheath boundary almost without collisions, and at low gas pressure a beam of fast electrons capable to ionize gas molecules emerges from the near-electrode sheath into the quasineutral plasma. The lower is the gas pressure, the more rare are collisions between electrons and gas molecules, the higher is the energy of electrons leaving the sheath, and the lower is the rf voltage which provides a sufficient number of high energy electrons to leave the sheath. That is, at low pressure the near-electrode sheath is not broken down (corresponding to $M<1$), however, the near-electrode sheaths serve as a source of fast electrons capable of ionizing gas molecules.

## V. CONCLUSIONS

The present paper studies the current-voltage characteristics (angle of phase shift between current and voltage, Ohmic current, and power absorbed by the discharge) of rf capacitive discharges in $N_2O$ at rf frequencies of 2 MHz, 13.56 MHz, and 27.12 MHz over a broad range of voltage and gas pressure. At 2 MHz the discharge is more Ohmic in nature, and the phase shift angle increases quickly with voltage and pressure. At low pressure (<0.2 Torr) the discharge can exist only in the strong-current $\gamma$-mode, whereas the weak-current $\alpha$-mode can also exist at higher $N_2O$ pressure. At 13.56 MHz and 27.12 MHz the discharge is more capacitive in nature, i.e., the phase shift angle is close to −90°. At these frequencies, above 0.75 Torr and at low rf voltage, the discharge can exist in the normal regime, whereas for 2 MHz the normal regime was not observed at all. The dependence of the Ohmic current on frequency in the weak-current mode at fixed voltage is satisfactorily described by the function $f^{5/3}$. The $\alpha-\gamma$ transition curves of the rf discharge at different rf frequencies were measured. A simple analytical treatment demonstrated that the $\alpha-\gamma$ transition corresponds to breakdown of the sheaths breakdown only for high gas pressure, whereas at low pressure this criterion is not met but the near-electrode sheaths in the $\gamma$-mode are a source of fast electrons.

[1] D. R. Lee, G. Lucovsky, M. S. Denker, and C. Magee, J. Vac. Sci. Technol. A **13**, 1671 (1995).
[2] S. R. Kaluri and D. W. Hess, J. Electrochem. Soc. **145**, 662 (1998).
[3] J. Campmany, J. L. Andujar, A. Canillas, J. Costa and E. Bertran, Appl. Surf. Sci. **70-71**, 695 (1993).
[4] J. Campmany, A. Canillas, J. L. Andujar, J. Costa and E. Bertran, Thin Solid Films **228**, 137 (1993).
[5] W. L. Scopel, R. R. Cuzinatto, M. H. Tabacniks, M. C. A. Fantini, M. I. Alayo, and I. Pereyra, J. Non-Cryst. Solids **288**, 88 (2001).
[6] M. I. Alayo, I. Pereyra, W. L. Scopel, and M. C. A. Fantini, Thin Solid Films **402**, 154 (2002).
[7] W. L. Scopel, M. C. A. Fantini, M. I. Alayo, and I. Pereyra, Thin Solid Films **413**, 59 (2002).
[8] G. Kaganowicz, V. S. Ban, and J. W. Robinson, J. Vac. Sci. Technol. A **2**, 1233 (1984).
[9] M. J. Kushner, J. Appl. Phys. **74**, 6538 (1993).
[10] C. H. Courtney, B. C. Smith, and H. H. Lamb, J. Electrochem. Soc. **145**, 3957 (1998).
[11] Y.-B. Park and S.-W. Rhee, J. Appl. Phys. **86**, 1346 (1999).
[12] J. Bandet, B. Despax, M. Caumont, and L. Date, Jpn. J. Appl. Phys., Part 1 **39**, L141 (2000).
[13] L. Date, K. Radouane, H. Caquineau, B. Despax, J. P. Couderc, and M. Yousfi, Surf. Coat. Technol. **116–119**, 1042 (1999).

[14]L. Date, K. Radouane, B. Despax, M. Yousfi, H. Caquineau, and A. Hennand, J. Phys. D **32**, 1478 (1999).
[15]L. E. Kline, W. D. Partlow, R. M. Young, R. R. Mitchell, and T. V. Congedo, IEEE Trans. Plasma Sci. **19**, 278 (1991).
[16]G. Francis, "The Glow Discharge at Low Pressure," in *Handbuch der Physik*, edited by S. Flugge (Springer, Berlin, 1956). Vol. XXII, p. 54.
[17]B. N. Klarfeld, L. G. Guseva, V. V. Vlasov, in Proceedings of the X International Conference on Phenomena in Ionized Gases, Oxford, Contributed Papers 1, p. 97 (1971).
[18]Y. P. Raizer, M. N. Shneider, N. A. Yatsenko, *Radio-Frequency Capacitive Discharges* (CRC Press, Boca Raton, 1995).
[19]V. A. Lisovskiy and V. D. Yegorenkov, J. Phys. D **31**, 3349 (1998).
[20]V. Lisovskiy, J.-P. Booth, S. Martins, K. Landry, D. Douai, and V. Cassagne, Europhys. Lett. **71**, 407 (2005).
[21]V. Lisovskiy, J.-P. Booth, K. Landry, D. Douai, V. Cassagne, and V. Yegorenkov, J. Phys. D **39**, 1866 (2006).
[22]N. A. Yatsenko, Sov. Phys. Tech. Phys. **26**, 678 (1981).
[23]N. A. Yatsenko, Sov. Phys. Tech. Phys. **33**, 180 (1988).
[24]V. A. Lisovskiy, Tech. Phys. **43**, 526 (1998).
[25]V. A. Lisovskiy and V. D. Yegorenkov, Vacuum **74**, 19 (2004).
[26]V. A. Godyak and A. S. Khanneh, IEEE Trans. Plasma Sci. **PS-14**, 112 (1986).
[27]P. Vidaud, S. M. A. Durrani, and D. R. Hall, J. Phys. D **21**, 57 (1988).
[28]Ph. Belenguer and J. P. Boeuf, Phys. Rev. A **41**, 4447 (1990).
[29]J. P. Boeuf and Ph. Belenguer, *Fundamental Properties of rf Glow Discharges: An Approach Based on Self-Consistent Numerical Models, in Nonequilibrium Processes in Partially Ionized Gases*, edited by M. Capitelli and J. N. Bardsley (Plenum, New York, 1990), p. 155.
[30]S. M. Levitskii, Sov. Phys. Tech. Phys. **2**, 887 (1958).